Afyon Kocatepe Üniversitesi Fen ve Mühendislik Bilimleri Dergisi
Afyon Kocatepe University – Journal of Science and Engineering
https://dergipark.org.tr/tr/pub/akufemubid

Araştırma Makalesi / Research Article
DOI: https://doi.org/10.35414/akufemubid.1345104
AKÜ FEMÜBİD **24** (2024) 025902 (457-464)
AKU J. Sci. Eng. **24** (2024) 025902 (457-464)

Effect of Mold Materials Used During Hot Embossing on Feature Fidelity for Microfabrication in Cyclic Olefin Polymer (COP) Substrate

Makale Bilgisi / Article Info
Alındı/Received: 23.08.2023
Kabul/Accepted: 07.03.2024
Yayımlandı/Published: 29.04.2024

Sıcak Kabartma Sırasında Kullanılan Kalıp Malzemelerinin Döngüsel Olefin Polimer (COP) Alttaşta Mikrofabrikasyonda Yapıların Doğruluğuna Etkisi

Ahmet Can ERTEN*
[1] *İstanbul Teknik Üniversitesi, Elektrik-Elektronik Fakültesi, Elektronik ve Haberleşme Mühendisliği Bölümü, İstanbul, Türkiye*

Abstract

During the transition from research to market, the fabrication of microfluidic devices in thermoplastic substrates is inevitable. For short production runs of several hundred products, hot embossing is the typical method before moving on to a typically more expensive injection molding process for higher production volumes. In this work, we investigated the effect of mold material used during hot embossing on feature fidelity for microfabrication in cyclic olefin polymer (COP) substrate. Specifically, we designed a simple flow-focusing microfluidic device and fabricated three different molds using silicon wafer by deep reactive ion etching (DRIE), aluminum filled high temperature epoxy by soft lithography and aluminum by CNC milling. We performed hot embossing experiments with 2mm thick COP substrates and these three different molds using automatic bench top Carver hot press. Finally, we characterized the hot embossed substrates by optical and scanning electron microscopy. Fabrication results demonstrate that the mold material plays a big role in feature fidelity. Among the mold materials used, silicon substrate performed the worst based on defects after demolding. Epoxy and aluminum molds were similar in terms of microfabricated feature defects in the substrate which could be mostly attributed to their coefficient of thermal expansion (CTE). A mold material with a CTE closer to the thermoplastic will result in much better feature fidelity.

Keywords *Hot Embossing; Cyclic Olefin Polymer; COP; Mold; Thermoplastic.*

Öz

Araştırmadan pazara geçiş sırasında, termoplastik yüzeylerde mikroakışkan cihazların imalatı kaçınılmazdır. Daha yüksek üretim hacimleri için tipik olarak kullanılan pahalı enjeksiyon kalıplama işlemine geçmeden önce birkaç yüz ürün gibi küçük hacimli üretim süreçleri için, sıcak kabartma tipik yöntemdir. Bu çalışmada, sıcak kabartma sırasında kullanılan kalıp malzemelerinin döngüsel olefin polimer (COP) substratta mikrofabrikasyonda üretim sonuçları üzerindeki etkisini araştırdık. Spesifik olarak, basit bir akış odaklamalı mikroakışkan cihazı tasarladık ve bu tasarımı kullanarak silisyum, alüminyum dolgulu epoksi ve alüminyum alttaşlar kullanarak üç farklı kalıp ürettik. Bu üç farklı kalıp malzemesini COP substrat ile otomatik tezgâh üstü Carver sıcak preste kullanarak sıcak kabartma deneyleri yaptık. Son olarak, sıcak kabartmalı alt tabakaları optik mikroskop ve taramalı elektron mikroskop ile karakterize ettik. Üretim sonuçları, kalıp malzemesinin üretim sonuçları üzerinde büyük bir rol oynadığını göstermektedir. Kullanılan kalıp malzemeleri arasında silisyum alttaş, kalıptan çıkarma sonrasındaki kusurlara göre en kötü performansı göstermiştir. Epoksi ve alüminyum kalıplar, çoğunlukla termal genleşme katsayılarına (CTE) atfedilebilen alt tabakadaki mikro fabrikasyon özellik kusurları açısından benzerdi. Termoplastiğe daha yakın bir CTE'ye sahip bir kalıp malzemesi, çok daha iyi özellik doğruluğu ile sonuçlanacaktır.

Anahtar Kelimeler *Sıcak Kabartma; Döngüsel Olefin Polimer; COP; Kalıp; Termoplastik.*

1. Introduction

Microfluidics has found many applications in diverse fields such as biology, chemistry, and material science (Liu and Jiang 2017; Sackmann et. al. 2014). With the introduction of soft lithography and the use of polydimethylsiloxane (PDMS) as a material, the popularity of microfluidics has increased thanks to the convenience of rapid prototyping in a lab environment without the need for expensive equipment (Duffy et al. 1998; Xia and Whitesides 1998). However, very few of those successfully demonstrated proof-of-concept laboratory prototypes ever made it into a successful commercial product (Blow 2009). One of the main reasons behind this low transferability of the prototypes into commercial products is the same reason that reduced the barrier to the development of microfluidic systems: PDMS. PDMS enabled fast and cheap prototyping of microfluidic systems but when eventually a successful prototype was

*Sorumlu Yazar/Corresponding Author: Ahmet Can Erten e-posta/e-mail: aerten@itu.edu.tr

demonstrated in PDMS, it needed to be manufactured in thermoplastics such as polymethyl methacrylate (PMMA), polycarbonate (PC), and polystyrene (PS) compatible with established cost-effective high-throughput manufacturing methods (Volpatti and Yetisen 2014).

Thermoplastics are a type of polymer that can be reshaped when heated near the glass transition temperature (Tg) of the material. They have several advantages including low material cost, availability of a range of material properties tailored for specific needs besides amenability for mass manufacturing (Becker and Locascio 2002). Besides many commonly used thermoplastics in microfluidics such as PMMA, PC and PS, cyclic olefin polymer (COP)'s high optical transparency, optical clarity, as well as low autofluorescence, and strong chemical resistance with low water absorption, make it an attractive material for microfluidic applications (Alrifaiy *et al.* 2012; Nunes *et al.* 2010).

Injection molding and hot embossing emerge as two popular high-throughput manufacturing methods for creating the desired channels in thermoplastics (Becker and Gärtner 2008; Fiorini and Chiu 2005; Rodrigues et al. 2015). Injection molding produces parts by injecting molten material into a mold. It is reproducible and low cost in high volume production cases. On the other hand, hot embossing - a process that involves pressing a patterned mold into a polymer sheet to create micro- or nano-scale features - is less expensive to set up for low to medium volume production making it practical choice for research labs (Berthier *et al.* 2012).

The success of the hot embossing process depends on the optimization of many parameters such as mold design and its material, thermoplastic and its Tg, compression force, embossing and demolding temperature and their durations (Cheng *et al.* 2014; Çoğun *et al.* 2017; Kourmpetis *et al.* 2019; Li *et al.* 2008; Sun et al. 2009). Typically, the mold material is one of the critical components of the hot embossing process that determines the quality and characteristics of the embossed structures obtained. For example, silicon molds patterned through deep reactive ion etching (DRIE) or KOH wet etching are common for their favorable surface finish and accuracy (Esch *et al.* 2003). Metal molds fabricated through electroplating and CNC machining are also preferred for their durability. Recently, high strength epoxy resin-based molds have been used for their more practical and low-cost fabrication (Koerner *et al.* 2005; Konstantinou *et al.* 2016). Besides these common mold materials, non-conventional mold materials such as PDMS and PMMA were also explored (Goral *et al.* 2011; Khan Malek *et al.* 2007; Liu *et al.* 2013; Liu *et al.* 2014). However, few studies have performed a direct comparison of these popular molds in terms of embossed feature accuracy (Jena *et al.* 2012; Konstantinou *et al.* 2016).

In this study, we designed a simple flow-focusing fluidic channel (Zhu and Wang 2017). We used hot embossing technique for replicating this design to COP material with three different mold materials i.e., silicon, aluminum and epoxy. We chose silicon molds for their familiarity to the microfluidics community and their potential for in-house development. We chose aluminum molds for their ease in bench-top milling systems and the short turn-around time required for their machining. Finally, we chose aluminum filled epoxy resin molds for the similarity of their fabrication process to the soft lithography process. Using a bench top hot press, we used the same hot embossing process with these different molds on pre-cut COP sheets. We investigated the role of mold materials on feature fidelity through assessment of embossed parts by optical microscopy and scanning electron microscopy (SEM).

2. Materials and Methods

2.1 Materials

Sylgard 184 base and curing agent were obtained from Dow Corning Corporation. PT4925A aluminum filled high-temperature epoxy resin and PT4925-B1 hardener were obtained from PTM&W Industries. COP substrates (Zeonor 1060R with glass transition temperate Tg of 100 ^{o}C) were obtained in 2mm thick sheets from Zeon Corporation. 4 inch 500 µm thick single side polished silicon wafers with <100> crystal orientations were obtained from University Wafer Corporation.

2.2 Fabrication of silicon mold

Initially, the schematics of a simple flow-focusing fluidic channel design with a minimum channel width of 100 µm and two alignment marks in the shape of plus signs (+) were drawn using CAD software and a high-resolution transparency mask was produced using a 4x2 array of this design. The schematic of the fluidic channels with 1.8mm inlets and approximately 25mm by 10mm bounding box is shown in Figure 1a. After a 10 µm thick positive resist layer was spin-coated onto a 4-inch single-side polished silicon wafer, the photoresist was patterned using photolithography process. The silicon mold was manufactured using a DRIE process with the resist acting as the etch mask to create features with approximately 40

µm height. Finally, once the features were defined in the silicon substrate, the remaining photoresist was removed using solvents and the wafer was diced to get about 30mm by 15mm molds.

2.3 Fabrication of epoxy mold

The epoxy mold was prepared similarly to the soft lithography process. First, PDMS was prepared by mixing Sylgard 184 base: curing agent at a ratio of 10:1. After degassing the PDMS mixture, it was poured over the silicon mold produced through DRIE etching and cured in oven at 65 ^{o}C for 3 hours. Next, the PDMS replica was used as the master for aluminum filled high-temperature epoxy resin PT4925 (PTM&W Industries, Santa Fe Springs, CA). PT4925 epoxy was prepared by mixing PT4925-A and PT4925-B1 at a ratio of 100:10 and cured at room temperature for 24 hours. After demolding from the PDMS mold, epoxy was post-cured for 4 hours at 65 ^{o}C followed by 4 hours at 120 ^{o}C and finally 4 hours at 175 ^{o}C in an oven. Finally, the mold was let to cool down to room temperature gradually.

2.4 Fabrication of aluminum mold

First, the schematics of the fluidic channels were converted into G-code using CAM software. Next, a small aluminum block was secured to the part holder of a 3-axis benchtop CNC mill and surfaced using a 1mm diameter flat end mill. Finally, a 100 µm diameter flat end mill was used for machining the aluminum mold.

2.5 Hot Embossing and Characterization

Hot embossing experiments were performed using an automatic benchtop hot press (Carver Auto 3889) with a clamping force capacity up to 15 tons. It was fitted with a 6-inch x 6-inch square heated platens and cooling was achieved by air and chiller water cooled platens.

First, the mold was placed on the bottom platen followed by carefully stacking the polymer substrate (25mm x 10mm x 2mm rectangular piece) on top of the mold. The mold and substrate were heated up to the polymer molding temperature. Specifically, the bottom platen and top platen were heated up to 110 ^{o}C (10^{o}C above Tg) and 90 ^{o}C (10^{o}C below Tg) respectively. The top and bottom plates were heated up to different temperatures to avoid excessive deformation in the 2mm thick COP substrate (Lee *et al.* 2010). When the constant molding temperature was reached, the top and bottom platens were moved towards each other until the pre-set maximum embossing force of 1 ton was achieved. Once the pre-set maximum embossing force was achieved, it was held at that value for a holding time of 3 minutes while the temperature was kept constant. After the holding time was complete, the demolding step started with the cooling of the bottom platen to 80 ^{o}C (20^{o}C below Tg) and top platen left at 90 ^{o}C (10^{o}C below Tg) while the embossing force was maintained. When the demolding temperature of the polymer was reached, the platens were moved to their initial position. Finally, the embossed thermoplastic part was demolded manually. After demolding, the manufactured parts and molds were investigated first using optical microscopy. A surface profilometry was used to obtain feature depths for the embossed COP parts as well. Next, the COP parts were diced into smaller pieces revealing fluidic channel cross-sections and their scanning electron microscopy (SEM) images were taken.

3. Results and Discussion

The mold had a significant influence on the accuracy of the embossed structures. The photographs of silicon, epoxy and aluminum molds showing the flow-focusing design are shown in Figure 1b, c and d respectively. The milling marks can be seen for the aluminum mold.

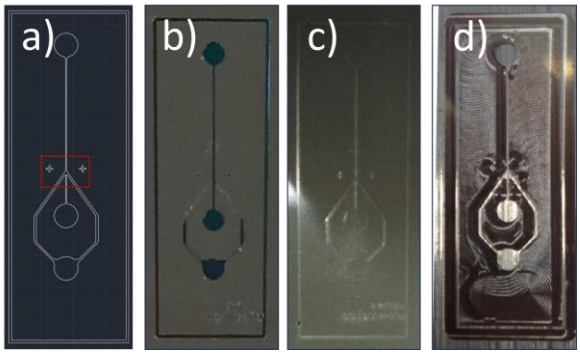

Figure 1. a) Schematic drawing of the mold (dashed red rectangle shows the flow focusing region with plus sign shaped alignment marks) b) Silicon mold c) Epoxy mold d) Aluminum mold

In Figure2a, a COP part embossed with the silicon mold is shown. The surface profilometry results of the COP part are shown in Figure2b and 2c. In Figure 2b, between points 1 and 2 (corresponding to approximately edges of the central fluidic inlet), the measured distance is around 1.75mm which is close to the designed diameter of 1.8mm. In Figure 2c, between points 3 and 4 (corresponding to the edges of the chip bounding box), the measured distance is around 0.15mm which is close to the designed distance of 0.2mm. For Figure2b and 2c, the embossed depth is around 37-38 µm which is in line with the silicon mold feature heights.

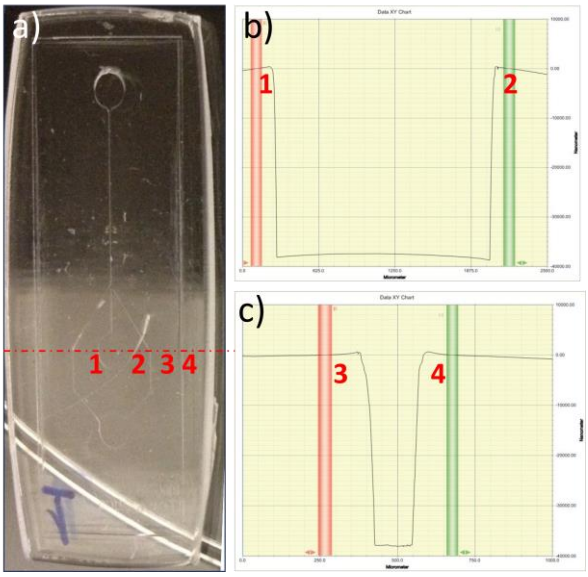

Figure 2. Surface profilometry results for the COP part hot embossed with the silicon mold. a) Photograph of the COP part hot embossed with the silicon mold (The section for which the surface profilometry was performed is shown with red line). b) The surface profilometry results for the section between points 1 and 2. c) The surface profilometry results for the section between points 3 and 4.

The close-up views of the flow-focusing regions (marked within the red dashed square in Figure 1a) with alignment marks for all three molds are shown in Figure 3a-c on the left. Among all three molds, the silicon mold shown in Figure 3a had the best surface finish in line with the reports in the literature. The epoxy mold shown in Figure 3b had the second-best surface finish with minor roughness due to the aluminum particles in the resin. Also, the epoxy mold had some minor defects around the alignment marks that happened during the demolding from the PDMS replica. The aluminum mold had the worst surface finish among the three molds with the milling marks visible as shown in Figure 3c. Moreover, the plus sign shaped alignment marks and the flow-focusing region had rounded corners due to the diameter of the end mill. The corresponding hot embossed COP substrates are shown in Figure 3a-c on the right. Here it can be seen that there are some defects visible as shadows in the optical microscopy images of the hot embossed parts which are not present on the molds themselves. The close-up views of the flow focusing region taken by SEM are shown in Figure 4. For the COP part embossed with silicon mold, local bulges around the left edge of the left channel and the right edge of the right channel are visible as shown in Figure 4a. These bulges were visible in Figure 3a as shadows. For the COP parts embossed with epoxy and aluminum mold, these bulges are not visible as shown in Figure 4b and 4c respectively.

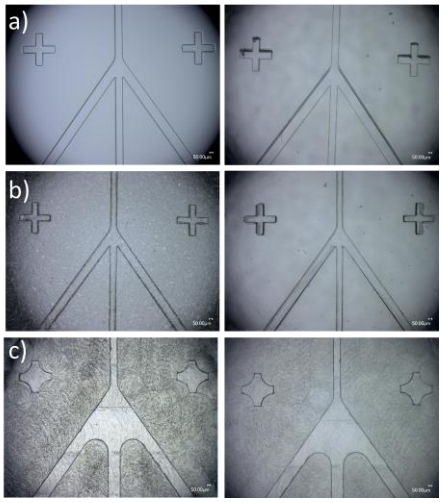

Figure 3. Close-up optical microscopy images of silicon, epoxy, aluminum molds, and corresponding hot embossed COP substrates. a) Silicon mold on the left and COP substrate on the right b) Epoxy mold on the left and COP substrate on the right c) Aluminum mold on the left and COP substrate on the right. (The scale bars at the bottom right corners correspond to 50 µm.)

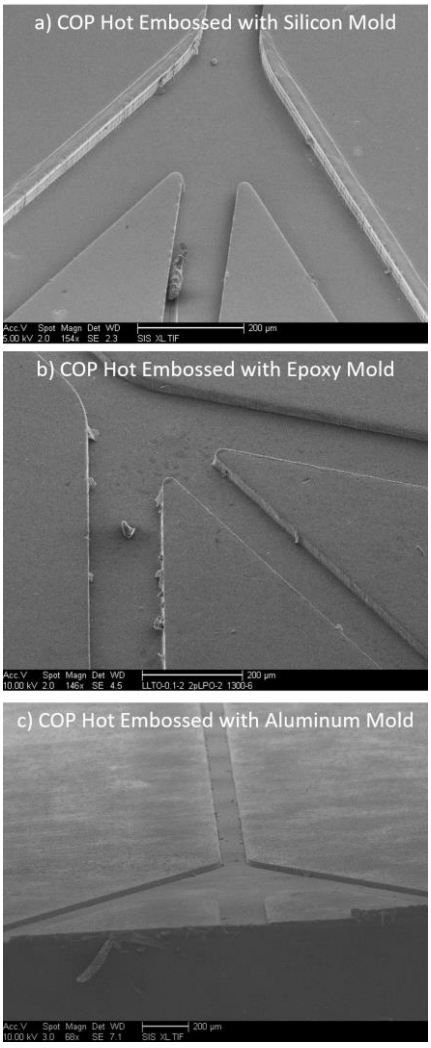

Figure 4. Close-up SEM images of hot embossed COP substrates. a) COP substrate hot embossed with the silicon mold b) COP substrate hot embossed with the epoxy mold c) COP substrate hot embossed with the aluminum mold. (The scale bars at the bottom correspond to 200 µm.)

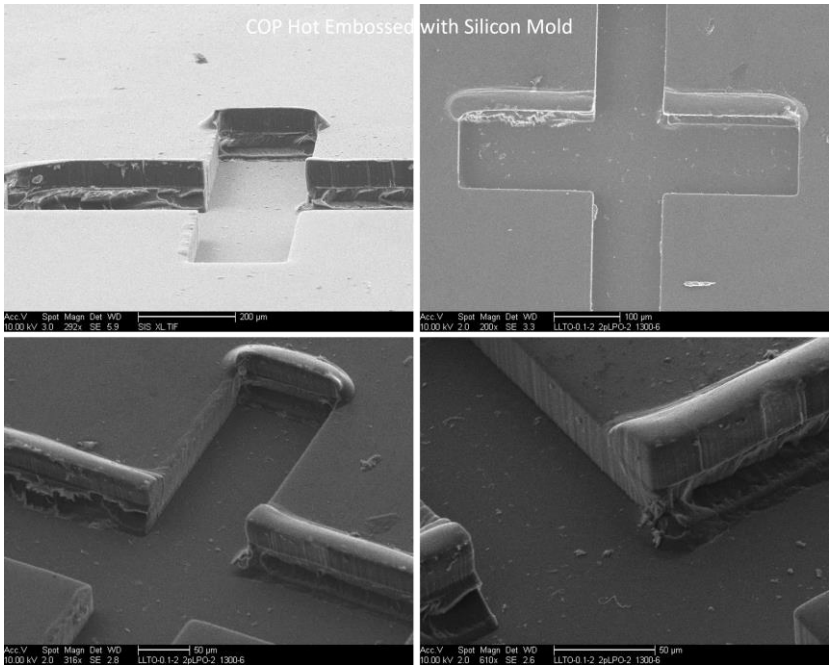

Figure 5. Close-up views of plus sign shaped alignment marks for COP part hot embossed with the silicon mold at different magnifications and from different perspectives.

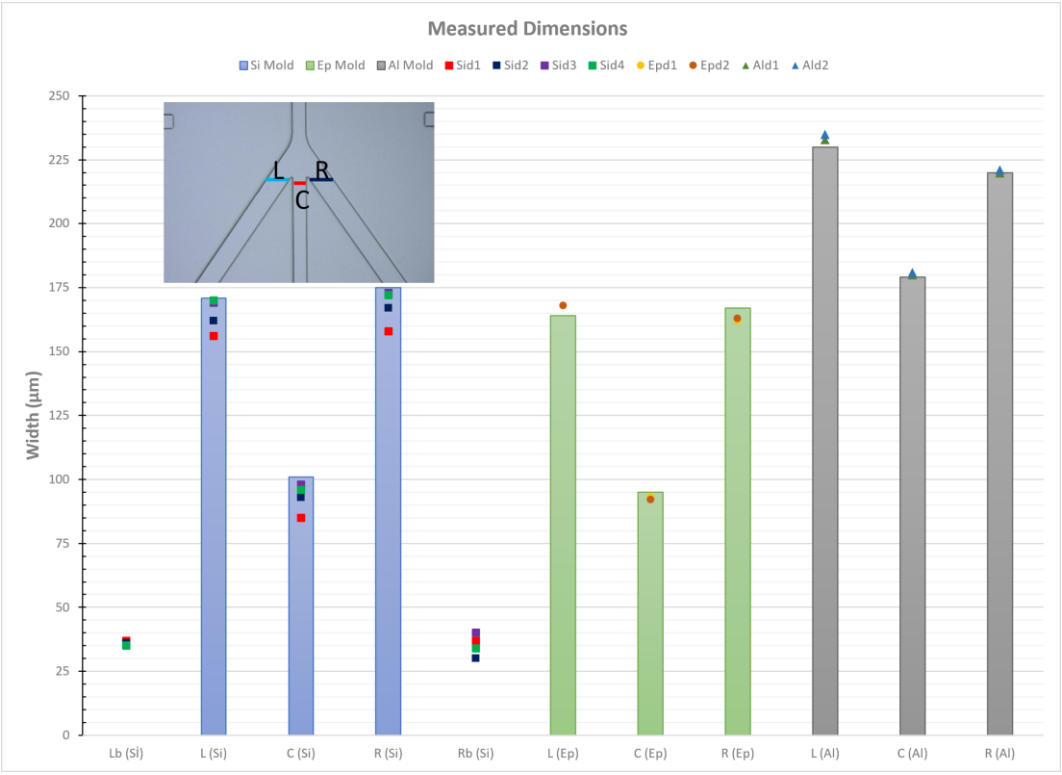

Figure 6. Measured dimensions of the silicon, epoxy and aluminum molds and hot embossed COP parts. The inset on the left shows the location of the measured regions. Lb and Rb represent the bulge widths on the left and right sides respectively. Mold dimensions are shown as columns.

The localization of the bulges only on the left edge of the left channel and the right edge of the right channel indicates the directionality of the defects. This directionality is more evident in Figure 5 in the plus sign shaped alignment marks of the COP part embossed with the silicon mold. In Figure 5, the plus sign shaped alignment mark images taken by SEM from different perspectives and magnifications are shown. The heights of the bulges are around 20 µm according to the SEM images.

In Figure 6, the measured dimensions of the silicon, epoxy and aluminum molds and hot embossed COP parts are plotted. The inset on the left shows the location of the measured regions. The region around the flow focusing

section where 3 channels merge was chosen due to the presence of bulges. The width of the left channel (L), central channel (C) and the right channel (R) as well as the bulges on the left channel (Lb) and the right channel (Rb) were measured. The measured dimensions for silicon, epoxy and aluminum molds were shown as columns. Silicon mold had dimensions closest to the schematic drawing with central channel width of around 101 µm (100 µm in schematics). The epoxy mold had a measured central width of around 95 µm and the difference between the original design and the measured dimension could be attributed mainly to the epoxy mold being made from PDMS replica. The aluminum mold had a measured central channel width of 179 µm. For all 4 COP parts hot embossed using silicon mold had bulges both on the left and the right side with an average bulge width of around 35 µm in the x direction and around 48 µm in the y direction. There were no significant bulges around the central channel. The COP parts hot embossed with epoxy and aluminum mold didn't have any significant bulges within the measured regions. The depth of the parts hot embossed with silicon, epoxy and aluminum parts were all measured to be around 30 µm. Bulges with a height of around 10 to 20 µm were present for the parts hot embossed with the silicon mold.

This directionality of the bulges can be attributed to the thermal expansion and contraction of mold and thermoplastic. As the temperature of the mold and the thermoplastic are raised, they expand in all directions symmetric to the center of the part according to the equation given in (1) where ΔL is the change in length, L_0 is the original length, ΔT is the temperature change and α is the linear coefficient of thermal expansion (CTE).

$$\frac{\Delta L}{L_0} = \alpha \Delta T \quad (1)$$

The CTE of some common mold materials and thermoplastics used in hot embossing are given in Table 1.

At the molding temperature, the mold is embossed into the thermoplastic part and after a certain embossing time, the system is cooled down to a temperature below the Tg and then manually demolded. During this cooling stage, the thermoplastic and the silicon mold try to contract proportionally with their CTE according to the formula given by (1) in all directions. However, the CTE of COP (70 µm/m ^{o}C) is much larger than the CTE of the mold material silicon (2.5 µm/m ^{o}C). Therefore, the COP tries to contract much more than silicon mold. While doing so, with the silicon mold still embossed into the COP part, COP pushes the silicon mold toward the center of the part. During this movement, the rigid silicon deforms the still relatively soft COP substrate forming bulges in the direction of its movement.

Table 1. Coefficient of linear thermal expansion (CTE) for some common mold materials and thermoplastics used in hot embossing process.

	Material	Coefficient of Thermal Expansion (m/m ^{o}C)
Mold	Silicon	2.5 x 10^{-6} Haynes (2014)
	Epoxy (PT4925A/B1)	56 x 10^{-6} [1]
	Aluminum	23 x 10^{-6} Haynes (2014)
	Stainless Steel	10-17 x 10^{-6} [2]
Thermoplastic	COP (Zeonor 1060R)	70 x 10^{-6} [3]
	PMMA	70 x 10^{-6} Haynes (2014)
	PC	68 x 10^{-6} Haynes (2014)

The bulges are not present in COP parts embossed with epoxy and aluminum molds. This could be attributed mainly to the CTE of aluminum (23 µm/m ^{o}C) and epoxy mold (56 µm/m ^{o}C) being very similar to the CTE of COP (70 µm/m ^{o}C). Another factor contributing to the presence of bulge defects in silicon mold is the relative ease of the mold movement with the COP substrate during the thermal contraction. The diced silicon mold is much thinner and therefore lighter than both the epoxy and the aluminum mold, aluminum mold being the thickest.

In order to avoid bulge defects, it is critical to choose a mold material with CTE close to the substrate material. In our case, both epoxy and aluminum molds were much better than the silicon mold. However, the aluminum mold has milling marks and it may be difficult to get sharp corners as was the case for our mold due to the radius of the milling bit. The epoxy mold was much better at replicating the flow focusing design, but the mold surface is still not as smooth as the silicon mold. Both aluminum and epoxy molds were more robust in terms of durability compared to the brittle silicon mold, aluminum being the best even though the dicing of the silicon mold into smaller parts helped with the durability of the mold, with less molds getting shattered during the demolding.

4. Conclusion

We have demonstrated that the mold material plays a critical role in the successful transfer of features on mold

via hot embossing on the desired substrate. Among the mold materials used, silicon substrate performed the worst based on defects after demolding. Epoxy and aluminum molds were similar in terms of microfabricated feature defects in the COP substrate which could be mostly attributed to their coefficient of thermal expansion (CTE). It was previously shown that the majority of defects in the hot embossing process can be reduced by optimizing the conditions for demolding. Here we validate the same conclusion with a study of different mold materials. In order to improve feature fidelity, it is critical to choose a mold material with CTE close to the substrate material.

Declaration of Ethical Standards
The authors declare that they comply with all ethical standards

Credit Authorship Contribution Statement
Author: Resources, Conceptualization, Investigation, Methodology, Data curation, Writing – original draft, Visualization

Declaration of Competing Interest
The authors declare that they have no known competing financial interests or personal relationships that could have appeared to influence the work reported in this paper.

Data Availability
All data generated or analyzed during this study are included in this published article.

Acknowledgement

The author wishes to thank Dr. Bernd Fruhberger, Dr. Xuekun Lu and Nano3 Cleanroom Facility for their support.

5. References

Alrifaiy, A., Lindahl, O. A. and Ramser, K., 2012. Polymer-based microfluidic devices for pharmacy, biology and tissue engineering. *Polymers*, **4**, 3. https://doi.org/10.3390/polym4031349

Becker, H. and Gärtner, C., 2008. Polymer microfabrication technologies for microfluidic systems. *Analytical and Bioanalytical Chemistry*, **390**, 1. https://doi.org/10.1007/s00216-007-1692-2

Becker, H. and Locascio, L. E., 2002. Polymer microfluidic devices. *Talanta*, **56**, 2. https://doi.org/10.1016/S0039-9140(01)00594-X

Berthier, E., Young, E. W. K. and Beebe, D., 2012. Engineers are from PDMS-land, biologists are from polystyrenia. *Lab on a Chip*, **12**, 7. https://doi.org/10.1039/C2LC20982A

Blow, N., 2009. Microfluidics: The great divide. *Nature Methods*, **6**, 9. https://doi.org/10.1038/nmeth0909-683

Cheng, G., Sahli, M., Gelin, J. C. and Barriere, T., 2014. Process parameter effects on dimensional accuracy of a hot embossing process for polymer-based micro-fluidic device manufacturing. *International Journal of Advanced Manufacturing Technology*, **75**, 1–4. https://doi.org/10.1007/s00170-014-6135-6

Çoğun, F., Yıldırım, E. and Sahir Arikan, M. A., 2017. Investigation on replication of microfluidic channels by hot embossing. *Materials and Manufacturing Processes*, **32**, 16. https://doi.org/10.1080/10426914.2017.1317795

Duffy, D. C., McDonald, J. C., Schueller, O. J. A. and Whitesides, G. M., 1998. Rapid prototyping of microfluidic systems in poly(dimethylsiloxane). *Analytical Chemistry*, **70**, 23. https://doi.org/10.1021/ac980656z

Esch, M. B., Kapur, S., Irizarry, G. and Genova, V., 2003. Influence of master fabrication techniques on the characteristics of embossed microfluidic channels. *Lab on a Chip*, **3**, 2. https://doi.org/10.1039/B300730H

Fiorini, G. S. and Chiu, D. T., 2005. Disposable microfluidic devices: Fabrication, function, and application. *BioTechniques*, **38**, 3. https://doi.org/10.2144/05383RV02

Goral, V. N., Hsieh, Y. C., Petzold, O. N., Faris, R. A. and Yuen, P. K., 2011. Hot embossing of plastic microfluidic devices using poly(dimethylsiloxane) molds. *Journal of Micromechanics and Microengineering*, **21**, 1. https://doi.org/10.1088/0960-1317/21/1/017002

Haynes, W. M., 2014. CRC handbook of chemistry and physics. CRC Press.

Jena, R. K., Yue, C. Y., Lam, Y. C., Tang, P. S. and Gupta, A., 2012. Comparison of different molds (epoxy, polymer and silicon) for microfabrication by hot embossing technique. *Sensors and Actuators, B: Chemical*, **163**, 1. https://doi.org/10.1016/j.snb.2012.01.043

Khan Malek, C., Coudevylle, J. R., Jeannot, J. C. and Duffait, R., 2007. Revisiting micro hot-embossing with moulds in non-conventional materials. *Microsystem Technologies*, **13**, 5–6. https://doi.org/10.1007/s00542-006-0184-1

Koerner, T., Brown, L., Xie, R. and Oleschuk, R. D., 2005. Epoxy resins as stamps for hot embossing of microstructures and microfluidic channels. *Sensors and Actuators, B: Chemical*, **107**, 2. https://doi.org/10.1016/j.snb.2004.11.035

Konstantinou, D., Shirazi, A., Sadri, A. and Young, E. W. K., 2016. Combined hot embossing and milling for medium volume production of thermoplastic microfluidic devices. *Sensors and Actuators, B: Chemical*, **234**. https://doi.org/10.1016/j.snb.2016.04.147

Kourmpetis, I., Kastania, A. S., Ellinas, K., Tsougeni, K., Baca, M., De Malsche, W. and Gogolides, E., 2019. Gradient-temperature hot-embossing for dense micropillar array fabrication on thick cyclo-olefin polymeric plates: An example of a microfluidic chromatography column fabrication. *Micro and Nano Engineering*, **5**. https://doi.org/10.1016/j.mne.2019.100042

Lee, C. S., Kang, C. G. and Youn, S. W., 2010. Effect of forming conditions on linear patterning of polymer materials by hot embossing process. *International Journal of Precision Engineering and Manufacturing*, **11**, 1. https://doi.org/10.1007/s12541-010-0015-2

Li, J. M., Liu, C. and Peng, J., 2008. Effect of hot embossing process parameters on polymer flow and microchannel accuracy produced without vacuum. *Journal of Materials Processing Technology*, **207**, 1–3. https://doi.org/10.1016/j.jmatprotec.2007.12.062

Liu, J., Jin, X., Sun, T., Xu, Z., Liu, C., Wang, J., Chen, L. and Wang, L., 2013. Hot embossing of polymer nanochannels using PMMA moulds. *Microsystem Technologies*, **19**, 4. https://doi.org/10.1007/s00542-012-1674-y

Liu, Y. and Jiang, X., 2017. Why microfluidics? Merits and trends in chemical synthesis. *Lab on a Chip*, **17**, 23. https://doi.org/10.1039/C7LC00627F

Liu, Y., Zhang, P., Deng, Y., Hao, P., Fan, J., Chi, M. and Wu, Y., 2014. Polymeric microlens array fabricated with PDMS mold-based hot embossing. *Journal of Micromechanics and Microengineering*, **24**, 9. https://doi.org/10.1088/0960-1317/24/9/095028

Nunes, P. S., Ohlsson, P. D., Ordeig, O. and Kutter, J. P., 2010. Cyclic olefin polymers: Emerging materials for lab-on-a-chip applications. *Microfluidics and Nanofluidics*, **9**, 2–3. https://doi.org/10.1007/s10404-010-0605-4

Rodrigues, R. O., Lima, R., Gomes, H. T. and Silva, A. M. T., 2015. Polymer microfluidic devices: An overview of fabrication methods. *U.Porto Journal of Engineering*, **1**, 1. https://doi.org/10.24840/2183-6493_001.001_0007

Sackmann, E. K., Fulton, A. L. and Beebe, D. J., 2014. The present and future role of microfluidics in biomedical research. *Nature*, **507**, 7491. https://doi.org/10.1038/nature13118

Sun, H. L., Liu, C., Li, M. M., Liang, J. S. and Chen, H. H., 2009. Study on replication of densely patterned, high-depth channels on a polymer substrate using hot embossing techniques. In *Materials Science Forum*. https://doi.org/10.4028/www.scientific.net/MSF.628-629.411

Volpatti, L. R. and Yetisen, A. K., 2014. Commercialization of microfluidic devices. *Trends in Biotechnology*, **32**, 7. https://doi.org/10.1016/j.tibtech.2014.04.010

Xia, Y. and Whitesides, G. M., 1998. SOFT LITHOGRAPHY. *Annual Review of Materials Science*, **28**, 1, 153–84. https://doi.org/10.1146/annurev.matsci.28.1.153

Zhu, P. and Wang, L., 2017. Passive and active droplet generation with microfluidics: a review. *Lab on a Chip*, **17**, 1. https://doi.org/10.1039/C6LC01018K

Internet References

1-https://www.ptm-w.com/technical-library/product-bulletins/Epoxy%20Tooling%20Materials%20Bulletins/PT4925%20Bulletin%2005Jul11.pdf, (02.01.2024)

2-https://www.engineeringtoolbox.com/linear-expansion-coefficients-d_95.html,(02.01.2024)

3-http://www.lookpolymers.com/polymer_Zeon-Chemicals-Zeonor-1060R-Cyclo-Olefin-Polymer.php, (02.01.2024)